





## RESEARCH ARTICLE

# Impairments in remote memory caused by the lack of Type 2 IP<sub>3</sub> receptors

António Pinto-Duarte<sup>1,2</sup>  | Amanda J. Roberts<sup>3</sup>  | Kunfu Ouyang<sup>4</sup>  | Terrence J. Sejnowski<sup>1,2,5</sup> <sup>1</sup>Computational Neurobiology Laboratory, Salk Institute for Biological Studies, La Jolla, California<sup>2</sup>Institute for Neural Computation, University of California San Diego, La Jolla, California<sup>3</sup>Animal Models Core Facility, The Scripps Research Institute, La Jolla, California<sup>4</sup>School of Chemical Biology and Biotechnology, State Key Laboratory of Chemical Oncogenomics, Peking University Shenzhen Graduate School, Shenzhen, China<sup>5</sup>Division of Biological Sciences, University of California San Diego, La Jolla, California**Correspondence**

António Pinto-Duarte and Terrence J. Sejnowski, Computational Neurobiology Laboratory, Salk Institute for Biological Studies, 10010 N Torrey Pines Road, La Jolla, CA 92037.

Email: antonio@snl.salk.edu (A. P.-D.) and terry@salk.edu (T. J. S.).

**Funding information**

Fundação Calouste Gulbenkian; Howard Hughes Medical Institute; Kavli Institute for Brain and Mind. Grant/Award Number: #2015-047; Shenzhen Basic Research Foundation, Grant/Award Numbers: KCYJ20160428154108239, KQJSCX20170330155020267

**Abstract**

The second messenger inositol 1,4,5-trisphosphate (IP<sub>3</sub>) is paramount for signal transduction in biological cells, mediating Ca<sup>2+</sup> release from the endoplasmic reticulum. Of the three isoforms of IP<sub>3</sub> receptors identified in the nervous system, Type 2 (IP<sub>3</sub>R2) is the main isoform expressed by astrocytes. The complete lack of IP<sub>3</sub>R2 in transgenic mice was shown to significantly disrupt Ca<sup>2+</sup> signaling in astrocytes, while leaving neuronal intracellular pathways virtually unperturbed. Whether and how this predominantly non-neuronal receptor might affect long-term memory function has been a matter of intense debate. In this work, we found that the absence of IP<sub>3</sub>R2-mediated signaling did not disrupt normal learning or recent (24–48 h) memory. Contrary to expectations, however, mice lacking IP<sub>3</sub>R2 exhibited remote (2–4 weeks) memory deficits. Not only did the lack of IP<sub>3</sub>R2 impair remote recognition, fear, and spatial memories, but it also prevented naturally occurring post-encoding memory enhancements consequent to memory consolidation. Consistent with the key role played by the downscaling of synaptic transmission in memory consolidation, we found that NMDAR-dependent long-term depression was abnormal in *ex vivo* hippocampal slices acutely prepared from IP<sub>3</sub>R2-deficient mice, a deficit that could be prevented upon supplementation with D-serine - an NMDA-receptor co-agonist whose synthesis depends upon astrocytes' activity. Our results reveal that IP<sub>3</sub>R2 activation, which in the brain is paramount for Ca<sup>2+</sup> signaling in astrocytes, but not in neurons, can help shape brain plasticity by enhancing the consolidation of newly acquired information into long-term memories that can guide remote cognitive behaviors.

**KEYWORDS**astrocyte, Ca<sup>2+</sup> signaling, behavior, long-term memory, synaptic plasticity

## 1 | INTRODUCTION

Astrocytes have vesicular compartments that are competent for Ca<sup>2+</sup>-dependent exocytosis of gliotransmitters, such as glutamate and Adenosine triphosphate (ATP), as well as the co-agonist of NMDA

Note added in proof: An independent report corroborating the ability of astrocytic signaling to modulate the strength of the CA3-CA1 synapse and remote, but not recent, memory has recently appeared in bioRxiv (Kol et al., 2019). In this elegant study, additional mechanistic insights on this topic are examined.

receptors, D-serine (Bezzi et al., 2004; Fiacco & McCarthy, 2004; Jourdain et al., 2007; Navarrete et al., 2012, 2013; Panatier et al., 2011; Takata et al., 2011; Zorec et al., 2016). We and others have shown that gliotransmitter release plays a role in neuronal network dynamics (Fellin et al., 2009; Lee et al., 2014), helping shape behaviors (Lee et al., 2014; Tanaka et al., 2013). However, due to the intimate morphological and structural organization of astrocytes and neurons in brain circuits, it is difficult to disentangle them, and the relevance of Gq G-protein-coupled

receptor–IP<sub>3</sub>R-mediated Ca<sup>2+</sup> signals (upstream of gliotransmitter release) to brain function and behavior has been questioned (Aguilhon et al., 2010; Petravicz et al., 2008; Petravicz et al., 2014). IP<sub>3</sub> is a second messenger broadly used by biological cells to regulate Ca<sup>2+</sup> release from the endoplasmic reticulum (Berridge, 1993; Foskett et al., 2007; Mikoshiba, 2007; Taylor & Tovey, 2010). Three IP<sub>3</sub> receptor subtypes (IP<sub>3</sub>R1, IP<sub>3</sub>R2, and IP<sub>3</sub>R3) have been identified in vertebrates, each of which displays distinct expression levels according to the type of cell (Foskett et al., 2007)—neurons and astrocytes are no exception, with IP<sub>3</sub>R1 and IP<sub>3</sub>R3 predominating in the former, and IP<sub>3</sub>R2 in the latter (Holtzclaw et al., 2002; Sharp et al., 1999). The expression of functional IP<sub>3</sub>R1 and IP<sub>3</sub>R3 in astrocytes has also been recently reported, but contrary to IP<sub>3</sub>R2-mediated Ca<sup>2+</sup> signals, which propagate over large territories, and thus are well placed to influence large populations of synapses, IP<sub>3</sub>R1 and IP<sub>3</sub>R3 receptors generate monophasic Ca<sup>2+</sup> events that are locally confined and do not propagate between astrocytic processes (Sherwood et al., 2017). Importantly, the full deletion of IP<sub>3</sub>R2 has proven ineffective in reducing intracellular Ca<sup>2+</sup> signals in neurons (Aguilhon et al., 2010; Di Castro et al., 2011; Petravicz et al., 2008; Takata et al., 2011).

Mice lacking IP<sub>3</sub>R2 have been shown to exhibit a reduction in the amplitude of astrocytic Ca<sup>2+</sup> oscillations, a decrease in their frequency and a complete absence of events with a large spatial spread (Okubo et al., 2019; Petravicz et al., 2008; Sherwood et al., 2017). Such astrocytic impairments were shown to reflect upon neural circuits, namely causing deficits upon cholinergic plasticity in the cerebral cortex (Takata et al., 2011) and hippocampus (Navarrete et al., 2012), but whether *Ip3r2*<sup>-/-</sup> mice display alterations upon cognitive processes has only been examined following photothrombosis-induced ischemia (Li et al., 2015), leaving such a core question largely outstanding. Notably, previous studies conducted in the IP<sub>3</sub>R2 KO mouse model have not found significant baseline alterations (i.e., in the absence of pharmacological stimulation) outside of the central nervous system that might suggest indirect influence on brain mechanisms (Li et al., 2005), deeming this mouse suitable for behavioral studies (Cao et al., 2013; Li et al., 2015). The experimental use of the IP<sub>3</sub>R2 KO mouse presents advantages over alternative methodologies targeting IP<sub>3</sub>R2 expression since this is the only model in which IP<sub>3</sub>R2 is completely absent in all astrocytes (cf. Petravicz et al., 2014; Tanaka et al., 2013). Moreover, similarly to a glial fibrillary acidic protein (GFAP)-dependent IP<sub>3</sub>R2 conditional KO (Petravicz et al., 2014), we have found that the IP<sub>3</sub>R2 KO displays normal health, lifespan, and exploratory behaviors, as well as unaltered learning and recent (24–48 h) memory, as we will later detail.

In contrast to the lack of effect on learning and recent memory, here we show that the absence of IP<sub>3</sub>R2 caused impairments in remote memory. Our evidence suggests that such an effect derived from a disruption of memory consolidation. Consistent with this hypothesis, we observed that long-term depression (LTD) recorded in acute hippocampal slices was impaired in this mouse compared to the wild type, a deficit that could be rescued by supplying exogenous D-serine to the extracellular medium. It is widely accepted that the combined effects of long-term potentiation (LTP) and LTD are essential to several long-term memory domains, including spatial memory (Bear & Abraham, 1996) and novelty recognition (Dong et al., 2012), with experience-dependent shifts in CA1

neurons selectivity requiring that neurons lose responsiveness to previously effective stimuli and acquire responsiveness to new stimuli through LTD and LTP, respectively (Bear & Abraham, 1996). It is also known that LTD enables the conversion of short-term to long-term memory (Dong et al., 2012) and plays an important role in memory consolidation (Ge et al., 2010), which might result from better information processing through the amplification of signal-to-noise ratio in potentiated synapses (Tononi & Cirelli, 2006). Taken together, our results demonstrate a previously unsuspected key contribution of IP<sub>3</sub>R2-mediated signaling to cognitive performance.

## 2 | MATERIALS AND METHODS

All animal procedures were performed in accordance with protocols approved by The Scripps Research Institute and the Salk Institute for Biological Studies' Institutional Animal Care and Use Committees (IACUC).

### 2.1 | Pharmacological drugs

D-serine and D-(-)-2-amino-5-phosphonopentanoic acid (D-AP5) were obtained from Tocris (Bio-Techne Corporation, Minneapolis, MN), and D-amino acid oxidase (DAAO) from porcine kidney was purchased from MilliporeSigma (St. Louis, MO).

### 2.2 | Animal model

*Ip3r2* heterozygous mutant (*Ip3r2*<sup>+/-</sup>) mice were originally generated on a mixed genetic background of Black Swiss, 129, and C57BL/6 (Li et al., 2005), and then backcrossed with C57BL/6 for three generations. *Ip3r2* null mutant (*Ip3r2*<sup>-/-</sup>) mice used in the experiments were then generated by intercrossing of *Ip3r2*<sup>+/-</sup> mice, and their wild-type (*Ip3r2*<sup>+/+</sup>) littermates were used as the control in all behavioral experiments and in some electrophysiological recordings, as indicated. In specific datasets involving electrophysiology experiments (where indicated), mice backcrossed to C57BL/6 for a total of no less than eight generations were obtained from a different colony, and the offsprings of homozygous crossings (*Ip3r2*<sup>-/-</sup> and *Ip3r2*<sup>+/+</sup>) were used as test and control, respectively. For the genotyping of littermates, we conducted protein-coupled receptor (PCR) analysis of mouse tail DNA with wild type (forward, GCTGTGCCAAAATCCTAGCACTG; reverse, CATGCAGAGGTCGTGTCAGTCATT) and mutant allele-specific primers (neo-specific primer: forward, AGTGATACAGGGCAAGTTCATAC; reverse, AATGGGCTGACCCTCCTCGT). The PCR conditions were: one cycle at 94°C 5 min, 36 cycles of 94°C 30 s, 60°C 30 s, 72°C 45 s, and a final extension step at 72°C for 5 min. PCR products were visualized following resolution in 1% agarose gel with ethidium bromide staining.

### 2.3 | Electrophysiological recordings

*Ip3r2*<sup>+/+</sup> (wt) and *Ip3r2*<sup>-/-</sup> mice (IP<sub>3</sub>R2 KO) of 25–37 days old were sacrificed under isoflurane anesthesia. When using littermates, the



experiments were conducted in genotypically different mice of the same sex, whenever possible. The brains were rapidly extracted and submerged in ice-cold aCSF containing (in mM): 130 NaCl, 2.5 KCl, 1.25 NaH<sub>2</sub>PO<sub>4</sub>, 24 NaCHO<sub>3</sub>, 10 glucose, 2 CaCl<sub>2</sub>, and 1.3 MgCl<sub>2</sub>, bubbled with 95% O<sub>2</sub> and 5% CO<sub>2</sub>, pH 7.4. The hippocampus was dissected free and slices (400 μm thick) were cut perpendicularly to the long axis of the hippocampus using a McIlwain tissue chopper. Hippocampal slices were allowed to recover functionally and energetically for at least 1 h in a resting chamber, filled with aCSF at room temperature (24–25°C).

Slices were transferred to a submerged recording chamber where they were continuously superfused (2 mL/min) with aCSF (same composition as above for LTP/depotential experiments or 0.65 mM MgCl<sub>2</sub> for all other protocols) at room temperature (24°C). Field excitatory postsynaptic potentials (fEPSPs) were evoked by stimulation of the Schaffer collateral–commissural fibers with rectangular pulses (0.1 ms wide for input–output curves, 0.2 ms for all other experiments) delivered through a concentric bipolar electrode (FHC, Inc. Bowdoin, ME) and recorded through an extracellular microelectrode (filled with aCSF, 2–6 MΩ resistance) placed in the *stratum radiatum* of the CA1 hippocampal region. Recordings were obtained with a Multiclamp 700 B amplifier, digitized at 10 kHz and filtered at 1–2 kHz. fEPSPs were evoked each 15 s (0.067 Hz) and stored on a personal computer with the WinLTP software (Anderson & Collingridge, 2007). fEPSPs were reduced to approximately 40–60% or 60–80% of the maximum amplitude before population spike contamination for LTP or LTD protocols, respectively, and stable baselines were collected for more than 15 min. LTD was induced by low-frequency stimulation (LFS, 1,000 stimuli at 1 Hz); LTP was induced by high-frequency tetanic stimulation (HFS, 100 Hz/1 s repeated four times at 15 s intervals). The depotential protocol was initiated 60 min after LTP induction using the same stimulation protocol as for LTD (LFS, 1,000 stimuli at 1 Hz). Effects on synaptic transmission were determined by calculating the percentage of fEPSP slope increase/decrease 54–60 min after the specific protocol, as compared to the last 10 min of baseline. Input–output curves were constructed by measuring fEPSPs slopes at increasing intensities (10–100 μA in 10 μA increments).

## 2.4 | Elimination of recessive retinal degeneration 1 mutation of the *Pde6b* gene for behavioral testing

The recessive retinal degeneration 1 mutation of the *Pde6b* gene known to be carried by the Swiss black background present in these mice (Li et al., 2005) could be a source of deficits in some behavioral tasks. We, therefore, screened the mice for this gene (Gimenez & Montoliu, 2001) and developed a breeding strategy that allowed us to successfully eliminate it before starting any behavioral testing. In brief, we used the following three independent oligonucleotides: RD3 (5'-TGA CAA TTA CTC CTT TTC CCT CAG TCT G-3'); RD4 (5'-GTA AAC AGC AAG AGG CTT TAT TGG GAA C-3'), and RD6 (5'-TAC CCA CCC TTC CTA ATT TTT CTC ACG C-3') to distinguish between the mutant *Pdebrd1* and wt allele at the *Pdeb* locus. The first pair of primers

(RD3/RD6) amplified a 0.40 kb PCR product from the wild-type allele, whereas no PCR product was expected from the *Pdebrd1* mutant allele, with the same experimental conditions. The second pair of primers (RD3/RD4) amplified a 0.55 kb PCR product from the *Pdebrd1* mutant allele. Finally, both PCR bands were present in heterozygous animals. The PCR conditions were: one cycle at 94°C 2 min, 35 cycles of 94°C 30 s, 65°C 30 s, 72°C 2 min, and a final extension step at 72°C for 10 min. PCR reaction was resolved in 1% agarose gel electrophoresis with ethidium bromide staining.

## 2.5 | Behavioral testing

Two cohorts of 29 male and female IP<sub>3</sub>R2 KO and wt mice (*n* = 6–10 per group per cohort) were tested. Behavioral experiments were conducted at the time points indicated in Table 1.

### 2.5.1 | General health, sensory, and neurological screen

This simple test allowed for the examination of general health and behaviors in mice. The first few measures were taken by observing each mouse in its home cage prior to any handling. These included an examination of coat condition, a check for barbered hair, piloerection, body tone, skin color, and limb tone. The home cage behavior prior to cage opening was also noted (i.e., solitary sleeping, nesting) and any evidence of fighting or aggression was noted. Each mouse was petted while still in the cage and it was noted if the mouse moved away. Then each mouse was lifted by the tail and its behavior was examined for passivity, trunk curl, and forepaw reaching. The mouse was scruffed for a firm hold and struggling and vocalization were noted. While scruffed, eye blink, ear twitch, whisker, and toe pinch reflexes, were assessed. The muzzle was examined for missing whiskers. A dowel was placed in front of the muzzle and biting behavior was scored. The mouse was then released onto a wire cage top. The top was slowly rotated so that the mouse was clinging upside down (if it was able to) and time to fall was recorded. Finally, the mouse was placed in an empty, clean cage, and freezing on transfer, wild running and stereotypies were noted if any and cage exploration was scored. The mouse was weighed and then returned to its home cage.

### 2.5.2 | Locomotor activity test

Locomotor activity was measured in polycarbonate cages (42 × 22 × 20 cm) placed into frames (25.5 × 47 cm) mounted with two levels of photocell beams at 2 and 7 cm above the bottom of the cage (San Diego Instruments, San Diego, CA). These two sets of beams allowed for the recording of both horizontal (locomotion) and vertical (rearing) behavior. A thin layer of bedding material was applied to the bottom of the cage. Mice were tested for 120 min and data were collected in 5-min intervals.

**TABLE 1** Number, weight (measured at 8 weeks for Cohort 1 and at 10 weeks for Cohort 2), and sex of mice ( $\delta$ : male;  $\varphi$ : female), behavioral test performed, and age of mice at testing (in weeks) in each cohort

Cohort	Animal numbers and weights (g)		Age at testing (in weeks)					
	Wt	IP <sub>3</sub> R2 KO	DLT	L	BM	YM	NOR	FC
1	$\delta$ (8) = 25.90 ± 0.9	$\delta$ (6) = 26.13 ± 1.6	9	9.5	10	13	-	14
	$\varphi$ (6) = 24.31 ± 1.7	$\varphi$ (9) = 22.32 ± 0.9						
2	$\delta$ (7) = 30.69 ± 3.5	$\delta$ (6) = 32.93 ± 3.5	-	-	12	11	17	20
	$\varphi$ (10) = 27.03 ± 2.0	$\varphi$ (6) = 25.65 ± 3.3						

Abbreviations: BM, Barnes maze (spatial learning/memory); DLT, dark–light transfer (anxiety); FC, fear conditioning (associative learning/fear memory); L, locomotor activity; NOR, novel object recognition (recognition memory); YM, Y-maze (working memory).

### 2.5.3 | Light/dark transfer test

The light/dark transfer procedure was used to assess anxiety-like behavior in mice by capitalizing on the conflict between exploration of a novel environment and the avoidance of a brightly lit open field. Our apparatus was a rectangular box made of Plexiglas divided by a partition into two environments. One compartment (14.5 × 27 × 26.5 cm) was dark (8–16 lux) and the other compartment (28.5 × 27 × 26.5 cm) was highly illuminated (400–600 lux) by a 60 W light source located above it. The compartments were connected by an opening (7.5 × 7.5 cm) located at floor level in the center of the partition. The time spent in the light compartment was used as a predictor of anxiety-like behavior, that is, a greater amount of time in the light compartment was indicative of decreased anxiety-like behavior. Mice were placed in the dark compartment to start the 5-min test.

### 2.5.4 | Optomotor

The optomotor allowed for assessment of visual ability. It consisted of a stationary elevated platform surrounded by a drum with black and white striped walls. Each mouse was habituated to the platform for 1 min and then the drum rotated at 2 rpm in one direction for 1 min, was stopped for 30 s and then rotated in the other direction for 1 min. The number of head tracks (15° movements at speed of drum) was recorded.

### 2.5.5 | Y-maze test for spontaneous alternations

Spontaneous alternations between the three arms in a Y-maze were taken as a measure of working memory. Single 5-min trials were initiated by placing each mouse in the center of the Y-maze. Arm entries were recorded with a video camera and the total number of arm entries, as well as the order of entries, was determined. Spontaneous alternations were defined as consecutive triplets of different arm choices.

### 2.5.6 | Barnes maze test

The Barnes maze, a spatial memory test very sensitive to impaired hippocampal function was used to study spatial learning and memory. The Barnes maze apparatus was an opaque Plexiglas disc 75 cm in diameter elevated 58 cm above the floor by a tripod. Twenty holes,

5 cm in diameter, were located 5 cm from the perimeter, and a black Plexiglas escape box (19 × 8 × 7 cm) was placed under one of the holes. Distinct spatial cues were located all around the maze and were kept constant throughout the study.

On the first day of testing, a training session was performed, which consisted of placing the mouse in the escape box for 1 min. After the habituation period, the first session was started. At the beginning of each session, the mouse was placed in the middle of the maze in a 10 cm high cylindrical black start chamber. After 10 s, the start chamber was removed, a buzzer (80 dB) and a light (400 lux) were turned on, and the mouse was set free to explore the maze. The session ended when the mouse entered the escape tunnel or after 3 min elapsed. When the mouse entered the escape tunnel, the buzzer was turned off and the mouse was allowed to remain in the dark for 1 min. When the mouse did not enter the tunnel by itself, it was gently put in the escape box for 1 min. The tunnel was always located underneath the same hole (stable within the spatial environment), which was randomly determined for each mouse. Mice were tested once a day for 9 days for the acquisition portion of the study.

For the 10th trial (probe test), on the following day, the escape tunnel was removed and the mouse was allowed to freely explore the maze for 3 min. The time spent in each quadrant was determined and the percentage of time spent in the target quadrant (the one originally containing the escape box) was compared with the percentage of time spent in the other three quadrants. This directly tested spatial memory, as there was no potential for local cues to be used by the mouse when making its decision.

Four weeks later (Cohort 1) or 2 weeks later (Cohort 2), the mice were tested again with the escape box placed in the original position (retention test). This allowed for the examination of remote memory.

Each session was videotaped and scored by an experimenter blind to the genotype of the mouse. Measures recorded included the latency to escape and the number of errors made per session. Errors were defined as nose pokes and head deflections over any hole that did not have the tunnel beneath it.

### 2.5.7 | Cued and contextual fear conditioning

Conditioning took place in Freeze Monitor chambers (Med Associates, Inc.) housed in soundproofed boxes. The conditioning chambers



( $26 \times 26 \times 17 \text{ cm}^3$ ) were made of Plexiglas with speakers and lights mounted on two opposite walls and shockable grid floors.

On Day 1, the mice were placed in the conditioning chambers for 5 min in order to habituate them to the apparatus. On Day 2, the mice were exposed to the context and conditioned stimuli (30 s, 3,000 Hz, 80 dB sound + white light) in association with foot shock (0.60 mA, 2 s, scrambled current). Specifically, the mice received two shock exposures in their 5-min test, each in the last 2 s of a 30-s tone/light exposure. On Day 3, contextual conditioning (as determined by freezing behavior) was measured in a 5-min test in the chamber where the mice were trained (context test). On the following day, the mice were tested for cued conditioning (CS+ test). The mice were placed in a novel context for 3 min, after which they were exposed to the conditioned stimuli (light + tone) for 3 min. For this test, the chamber was disguised with new walls (white opaque plastic creating a circular compartment in contrast to a clear plastic square compartment) and a new floor (white opaque plastic in contrast to the metal grid). Freezing behavior (i.e., the absence of all voluntary movements except breathing) was measured in all of the sessions by real-time digital video recordings calibrated to distinguish between subtle movements, such as whisker twitches, tail flicks, and freezing behavior. Freezing behavior in the context and cued tests (relative to the same context prior to shock and an altered context prior to tone, respectively) was indicative of the formation of an association between the particular stimulus (either the environment or the tone) and the shock; that is, that learning had occurred. This procedure was repeated in a second cohort, except that the context and CS+ tests occurred 30 days following conditioning.

### 2.5.8 | Novel object recognition test

The novel object recognition (NOR) test was used to assess the ability to recognize novelty in the environment. Mice were individually habituated to a  $51 \text{ cm} \times 51 \text{ cm} \times 39 \text{ cm}$  open field for 5 min. For the familiarization trials, two plastic toy objects were placed in the open field (one in each of two corners), and an individual animal was allowed to explore for 5 min. This was repeated with the same objects in the same locations another five times (separated by 1 min in a holding cage). Two weeks later each mouse was tested in an object novelty recognition test in which a novel object replaced one of the familiar objects. All objects and the arena were thoroughly cleaned with 70% ethanol between trials to remove odors. The three different objects required for this study were chosen based on there being no statistically significant preference for any object in pilot studies using C57BL/6J mice. These included a toy farmer boy, cow, and queen (Playmobil, Geobra Brandstatter GmbH & Co. KG, Zirndorf, Germany). The objects chosen were made of durable nontoxic plastic and were fixed to  $10 \text{ cm} \times 7 \text{ cm} \times 0.5 \text{ cm}$  square clear Plexiglas bases to prevent mice from moving the objects during testing. "Exploration" was defined as approaching the object nose-first within 2–4 cm. The number of approaches toward each object was calculated for each trial. Habituation to the objects across the five familiarization trials (decreased contacts) was an initial measure of learning; renewed interest (increased contacts) in the new object indicated evidence of object memory.

## 2.6 | Statistical analysis

Behavioral data were subjected to two-way analysis of variances (ANOVAs) with the genotype and sex as independent variables and the measure corresponding to a specific test as the dependent variable. In specific cases, as indicated, significant effects were further explored with lower level ANOVAs. Electrophysiological data were subjected to ANOVA followed by the Bonferroni correction in the case of multiple group comparisons or to Student's *t* test when comparisons were made between two groups. A critical value for significance of  $p < .05$  was used throughout the study. All data are expressed as the mean  $\pm$  SEM of *n* experiments.

## 3 | RESULTS

We started by assessing the overall health, sensory, and neurological features of the *Ip3r2*<sup>-/-</sup> mouse. We did not find significant differences between IP<sub>3</sub>R2 KO mice and the wt littermates used as a control, including in weight (Table 1) and coat condition (see section 4). Nor were there alterations in ambulatory activity, center activity, total horizontal activity (Figure 1a–c), or rearing (data not shown) related to genotype. Next, we confirmed using the optomotor, that all mice could see and that there were no significant differences in visual ability between groups (Figure 1d). Similarly, we did not find appreciable differences in anxiety levels between IP<sub>3</sub>R2 KO mice and wt littermates, as assessed using the dark–light transfer test: the time spent by IP<sub>3</sub>R2 KO mice in the light compartment (Figure 1e) and the number of transitions between dark and bright compartments (data not shown) were not significantly different compared to control animals. We also analyzed the capacity of the IP<sub>3</sub>R2 KO to store and manipulate recently acquired spatial information (working memory) as a function of the number of spontaneous alternations in the three arms Y-maze. Data from two cohorts of mice combined revealed that *Ip3r2*<sup>-/-</sup> made slightly less spontaneous alternations than wt mice (Figure 1f;  $F[1,54] = 5.64$ ,  $p < .05$ ), while there were no genotypic differences in the total number of arm entries (data not shown). The small magnitude of that effect (<5%), which was only present in one of the cohorts when analyzed separately, suggests that while the lack of IP<sub>3</sub>R2-mediated signaling might act to fine-tune working memory, it does not disrupt it in a critical manner.

The absence of major abnormalities in noncognitive behaviors and in working memory in IP<sub>3</sub>R2 KO mice established an adequate baseline for investigating the role played by IP<sub>3</sub>R2-mediated signaling in cognitive behaviors requiring learning and long-term memory employment.

### 3.1 | IP<sub>3</sub>R2-mediated Ca<sup>2+</sup> signaling contributed to long-term memory

In a previous collaboration (Lee et al., 2014), we observed that mice with astrocytes that were genetically engineered to express tetanus neurotoxin (TeNT) — a peptide that inhibits vesicular release, displayed significant deficits in recognition memory. This type of episodic memory

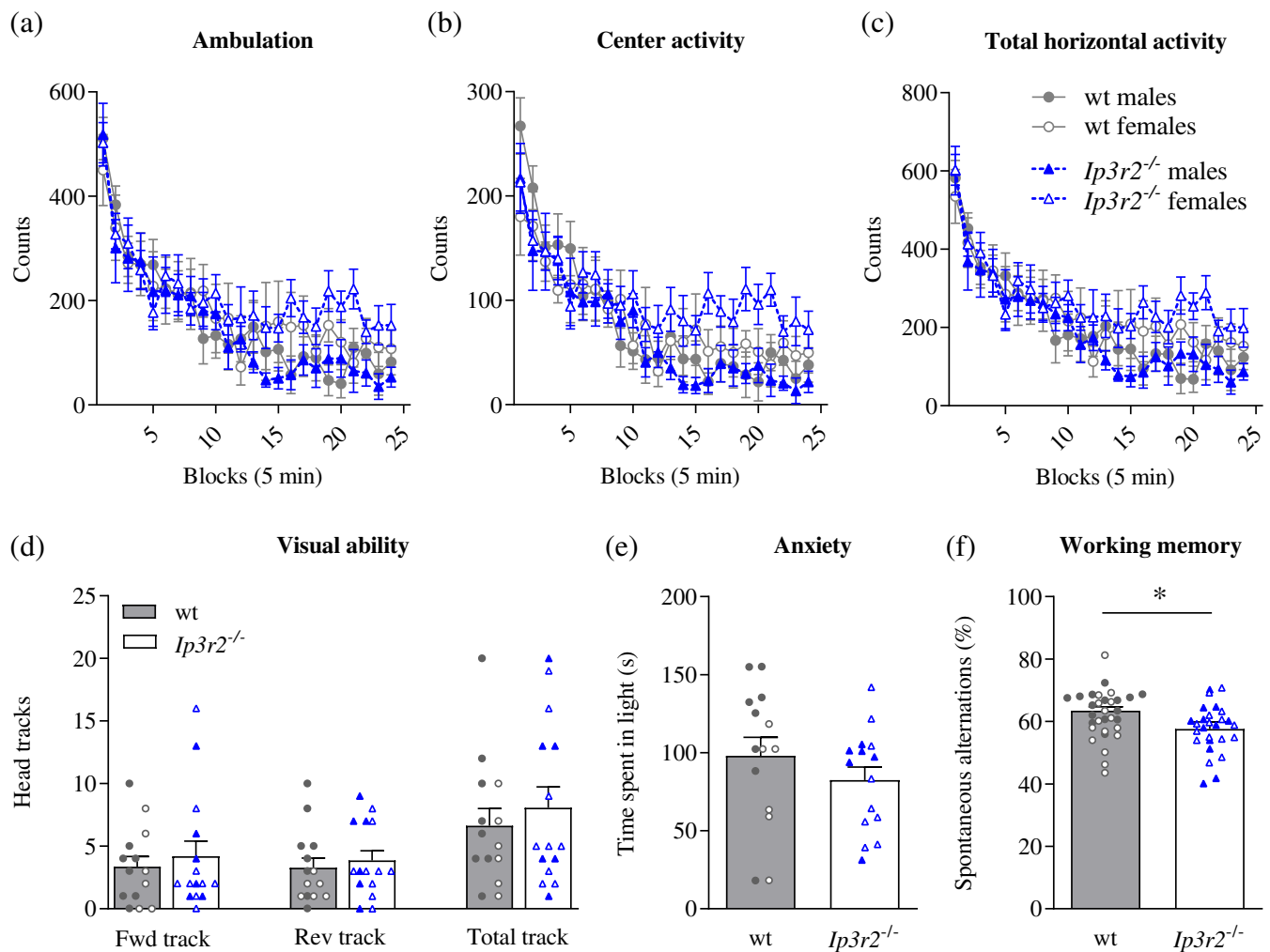


**FIGURE 1** Characterization of passive behaviors in IP3R2-deficient mice. *Ip3r2*<sup>-/-</sup> mice and wt littermate controls displayed normal ambulatory behavior (a), center activity (b), and total horizontal activity (c). *Ip3r2*<sup>-/-</sup> mice and wt littermate controls exhibited similar performances in the optomotor, being able to follow the moving stripes in the direction in which they were presented, as assessed by the number of forward (Fwd) and reverse (Rev) head tracks (d). On average, mice of both genotypes also performed similarly in the dark–light transfer test, spending comparable amounts of time in the light compartment (e). The percentage of spontaneous alternations in the Y-maze, measured as the consecutive triplets of different arm choices divided by the total number of arm entry triplets, was slightly reduced ( $*p < .05$ ) in *Ip3r2*<sup>-/-</sup> compared to wild-type mice (f). Graphs represent mean  $\pm$  SEM. Individual experiments are superimposed on bar graphs with open and closed symbols (circles, wt; triangles, *Ip3r2*<sup>-/-</sup> mice) representing females and males, respectively [Color figure can be viewed at [wileyonlinelibrary.com](http://wileyonlinelibrary.com)]

engages the hippocampus, as well as other brain areas, such as the perirhinal cortex and raphe nuclei, and it can be quantified experimentally using the novel object recognition (NOR) test. In this test, which has been shown to be particularly sensitive to alterations in hippocampal function (Broadbent et al., 2010), mice are expected to discriminate a novel object from an object for which they already have a mental representation (familiar object), by increasing the number of contacts with the former. Concurring with our previous collaborative study using the GFAP-tetanus toxin mouse (Lee et al., 2014), we observed that, overall, IP<sub>3</sub>R2 KOs were significantly less interested in a novel object, compared to controls (Figure 2a, right panel;  $F[1,25] = 5.8$ ,  $p < .05$ ). Although such an effect was driven mostly by female mice (Figure 2a, right panel), the number of contacts made by each individual mouse with the novel object, relative to the final familiarization trial, was significantly increased ( $p < .05$ ,

paired Student's *t* test) in both female ( $6.3 \pm 2$  vs.  $19.1 \pm 3$ ,  $n = 10$ ) and male ( $1.6 \pm 0.9$  vs.  $12.9 \pm 3$ ,  $n = 7$ ) wt mice, while it failed to reach statistical significance in female ( $2.8 \pm 0.9$  vs.  $4.2 \pm 1$ ,  $n = 6$ ) and male ( $6.8 \pm 3$  vs.  $13.3 \pm 1$ ,  $n = 6$ ) IP<sub>3</sub>R2 KO mice. The number of contacts with the familiar object was not significantly different between genotypes during the habituation period (Figure 2a,b, left panels), nor during a probe trial carried out 2 weeks later (Figure 2b, right panel).

### 3.2 | Lack of IP3R2-mediated signaling induced deficits in multiple types of remote, but not recent, long-term memory

In order to investigate whether the effects of IP<sub>3</sub>R2-mediated signaling were only linked to recognition memory, as in the case of the TeNT

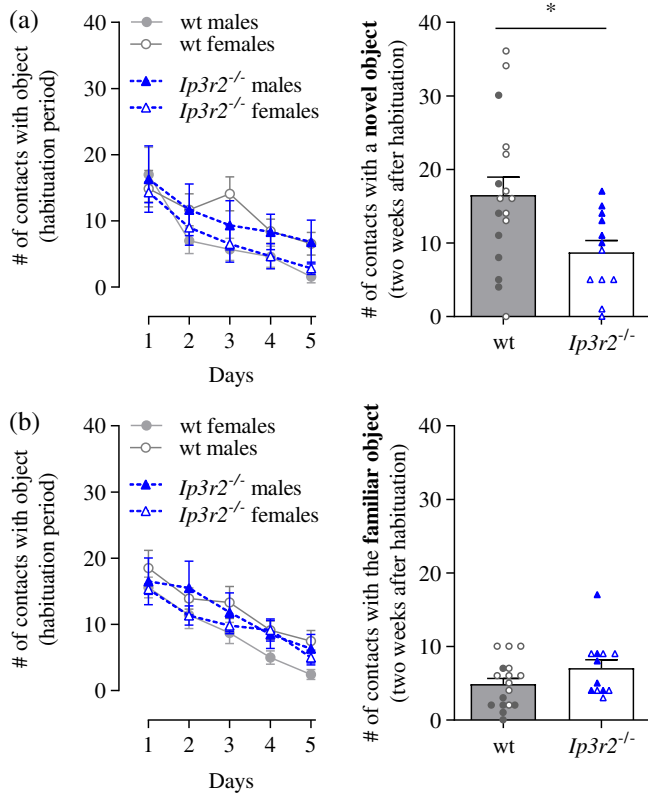


**FIGURE 2** Long-term recognition memory was impaired in *Ip3r2*<sup>-/-</sup> mice. *Ip3r2*<sup>-/-</sup> and wt littermate control mice became equally familiarized with two objects during the habituation period, as suggested by the comparable decrease in the number of contacts made with those objects between trials 1–5 at consecutive days (a and b, left panels). When presented with a novel object 2 weeks later, wt mice made a significantly greater number of contacts with that object ( $*p < .05$ ), as compared with their *Ip3r2*<sup>-/-</sup> littermates (a, right panel). There was no genotypic difference in the number of contacts with the familiar object 2 weeks after the habituation took place (b, right panel). Data represent mean  $\pm$  SEM. Individual experiments are superimposed on bar graphs with open and closed symbols (circles, wt; triangles, *Ip3r2*<sup>-/-</sup> mice) representing females and males, respectively [Color figure can be viewed at [wileyonlinelibrary.com](http://wileyonlinelibrary.com)]

mouse (Lee et al., 2014), or if, otherwise, those could facilitate memory function more broadly, we performed a comprehensive set of cognitive tests, including fear-conditioning experiments. For this purpose, we used methods that allowed testing recent and remote memory, as well as hippocampal- and amygdala-dependent learning processes in the same mouse. In these procedures, mice learned to associate a novel environment (context) and previously neutral stimuli (conditioned stimuli, a tone and a light) with an aversive foot shock stimulus. Testing then occurred in the absence of the aversive stimulus. Conditioned animals, when exposed to the conditioned stimuli, tended to refrain from all but respiratory movements by freezing. Freezing responses were triggered by exposure to either the context in which the shock was received (context test) or the conditioned stimuli (CS+ test). In our experiments, both genotypes of Cohort 1 had successful contextual and cued conditioning and there were no statistically significant differences between *IP<sub>3</sub>R2* KO and wt

mice when the context and CS+ trials occurred 24 and 48 h following conditioning (recent memory, Cohort 1; Figure 3a). In contrast, when trials were conducted 30 days after conditioning, *IP<sub>3</sub>R2* KO mice showed decreased freezing relative to wt mice in both the context and CS+ test (remote memory, Cohort 2; Figure 3b). Likely due to the high level of variability, the difference was not statistically significant in the context test, as it was in the CS+ test ( $F[1,25] = 5.5, p < .05$ ). These results are consistent with the finding of a deficit in long-term memory in *IP<sub>3</sub>R2* KO mice—specifically in remote memory.

The putative involvement of *IP<sub>3</sub>R2*-mediated signaling in hippocampus-dependent memory was significantly clearer when we used a spatial-reference task, the Barnes maze, which has the benefit of minimizing distress to the animal, compared to other hippocampal-dependent spatial tests involving more aversive conditions, such as the Morris water maze.

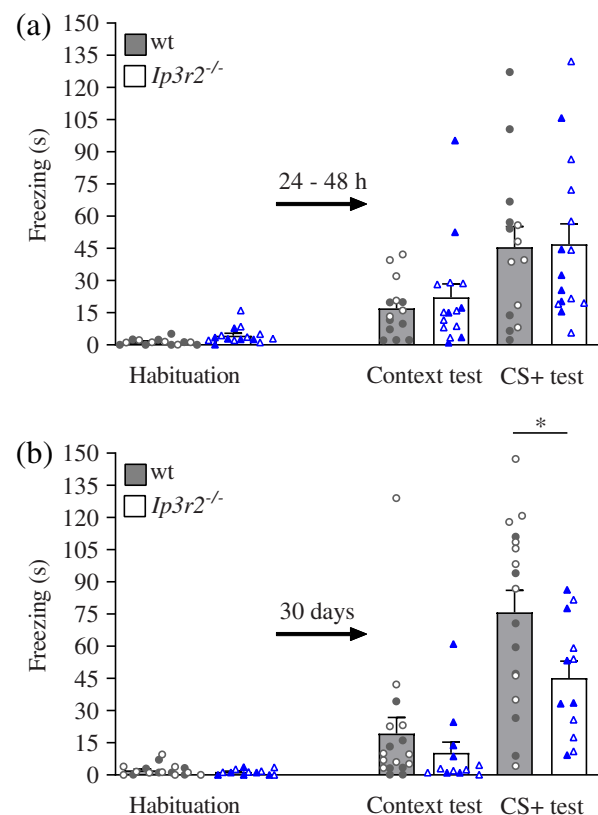


**FIGURE 3** Only remote, and not recent, fear memory was impaired in *Ip3r2*<sup>-/-</sup> mice. Wt and *Ip3r2*<sup>-/-</sup> littermates learned to associate sensory cues (tone + light) with a foot shock. Then, 1–2 days (a, recent memory) or 30 days later (b, remote memory), the freezing responses could be evoked in the absence of the foot shock by simply exposing the mice to either the context in which the shock was received (context test) or the cues (conditioned stimuli, CS+ test). Note that *Ip3r2*<sup>-/-</sup> mice showed decreased freezing time as compared to wt both in the context and CS+ tests only when remote memory was tested (b); likely due to the high variability observed, such differences were only statistically significant in the CS+ test ( $*p < .05$ ). Data represent mean  $\pm$  SEM. Individual experiments are superimposed on bar graphs with open and closed symbols (circles, wt; triangles, *Ip3r2*<sup>-/-</sup> mice) representing females and males, respectively [Color figure can be viewed at [wileyonlinelibrary.com](http://wileyonlinelibrary.com)]

During a 9-day training period in the Barnes maze, there were no significant differences between  $IP_3R2$  KO and wt littermates in escape latencies (Figure 4a), nor in the number of errors made (Figure 4b) when trying to find the escape chamber. Similarly, we did not find differences in recent memory, when we conducted the probe trial on the day that immediately followed the training period (Figure 4c). However,  $Ip3r2^{-/-}$  mice made significantly more errors than wt littermates when retested 2 weeks (Figure 4d,  $F[1,25] = 5.3, p < .05$ ) or 4 weeks later (Figure 4d,  $F[1,24] = 4.73, p < .05$ ) in different cohorts. Further analysis of the two cohorts combined showed that  $IP_3R2$ -related impairments were also expressed in male mice ( $F[1,53] = 4.38, p < .05$  for male wt vs. male  $Ip3r2^{-/-}$  and female wt vs. male  $Ip3r2^{-/-}$  animals, one-way ANOVA). Taken together with the results described above, these suggest that the lack of  $IP_3R2$  was deleterious for both female and male mice.

Although relatively modest if considered individually, the differences observed in the multiple behavioral tests described above all converge in support of the finding that the lack of  $IP_3R2$ -mediated  $Ca^{2+}$  signaling disrupts remote memory. This made us ponder whether such an impairment might derive from defective memory consolidation or retrieval, with our data supporting the former, as detailed below.

### 3.3 | Remote memory impairment in the $Ip3r2^{-/-}$ mouse stemmed from deficient memory consolidation

As Figure 4e indicates, there was a significant improvement ( $p < .05$ , paired Student's  $t$  test) in spatial memory when we retested our wild-type mice following a period of absence of stimulation (2–4 weeks).

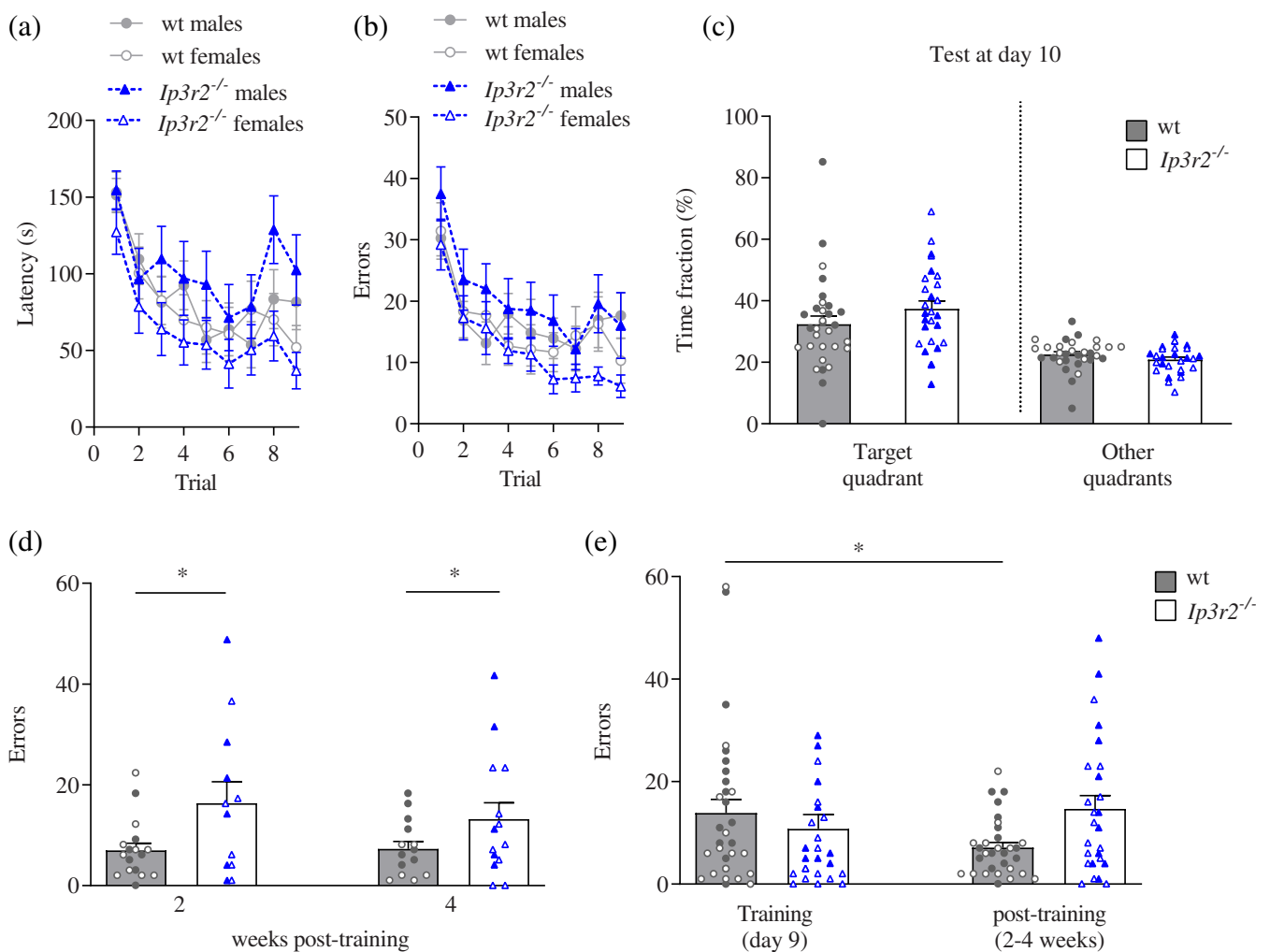


**FIGURE 4** Remote, but not recent, spatial memory was disrupted in  $Ip3r2^{-/-}$  animals. Learning curves were similar between  $Ip3r2^{-/-}$  and wt littermates, as assessed by the latencies (a) and the number of errors (b) made across the 9 days of the acquisition phase of the Barnes maze. Moreover, when the animals were probed at Day 10, there were no significant differences in the time spent by the animals at the target quadrant (c), which suggests normal learning. However, when a temporal delay (2–4 weeks) was introduced between the learning and retesting phases,  $Ip3r2^{-/-}$  mice made significantly more errors ( $*p < .05$ ) than their wt littermate controls when trying to find the escape chamber (d). Also note that the 2–4 weeks delay allowed wt mice to perform significantly better compared to the last day of training ( $*p < .05$ ), whereas such improvement was not observed in  $Ip3r2^{-/-}$  animals (e). Data represent mean  $\pm$  SEM. Individual experiments are superimposed on bar graphs with open and closed symbols (circles, wt; triangles,  $Ip3r2^{-/-}$  mice) representing females and males, respectively [Color figure can be viewed at [wileyonlinelibrary.com](http://wileyonlinelibrary.com)]



Such a capacity to outperform the last day of training, which was absent in the IP<sub>3</sub>R2 KO, is a well-known byproduct of memory consolidation, in which hippocampal LTD (Marshall & Born, 2007; Tononi & Cirelli, 2003, 2006) and the reactivation of the hippocampus during slow-wave sleep (Buzsáki, 1998; Diekelmann & Born, 2010; Lee & Wilson, 2002) play an active role. Recently, Foley et al. (2017) showed that the attenuation of IP<sub>3</sub>/Ca<sup>2+</sup> signaling in astrocytes did not impact slow-wave sleep, leaving out the possibility that IP<sub>3</sub>R2 deletion might affect LTD, which we sought to investigate next by recording fEPSPs in the CA1 region of acutely prepared hippocampal slices upon stimulation of the Schaffer collateral fibers (Figure 5a).

We applied LFS (1 Hz) to the Schaffer collaterals in order to induce N-methyl-D-aspartate receptor (NMDAR)-dependent LTD. In spite of observing a similar depression at the end of the LFS paradigm (wt: 41.1 ± 2% vs. IP<sub>3</sub>R2 KO: 37 ± 2%, Figure 5b), LTD maintenance (measured 1 h later) was significantly compromised in the IP<sub>3</sub>R2 KO (5.2 ± 2%, *n* = 15 slices, 14 mice) compared to wt mice (16.9 ± 2%,

*n* = 15 slices, 15 mice; Figures 5b). We then wondered whether this impairment could be rescued by adding to the bathing solution the obligatory co-agonist of NMDA receptors, D-serine, which has been shown to be released by astrocytes during LFS (Zhang et al., 2008), and which has been positively correlated with the expression of IP<sub>3</sub>R2 (Takata et al., 2011). In line with our hypothesis, we observed that in aCSF supplemented with D-serine (10 μM; Zhang et al., 2008), the average LTD measured 1 h after LFS was practically indistinguishable between wt (13.8 ± 4%, *n* = 8 mice) and IP<sub>3</sub>R2 KO (14.3 ± 3%, *n* = 10 slices, 9 mice; Figures 5c,d).

In a new set of experiments, we tested the robustness of our findings, while aiming to gain further mechanistic insights onto IP<sub>3</sub>R2-dependent modulation of LTD. To achieve this, we prepared hippocampal slices from *Ip3r2*<sup>-/-</sup> and wild-type mice derived from a different colony, and subjected them, as before, to LFS. Consistent with our previous observations, as shown in Figure 6, slices from *Ip3r2*<sup>-/-</sup> animals showed significantly reduced LTD compared to wild type (*Ip3r2*<sup>-/-</sup>: 7.4 ± 2% vs. wt: 20.0

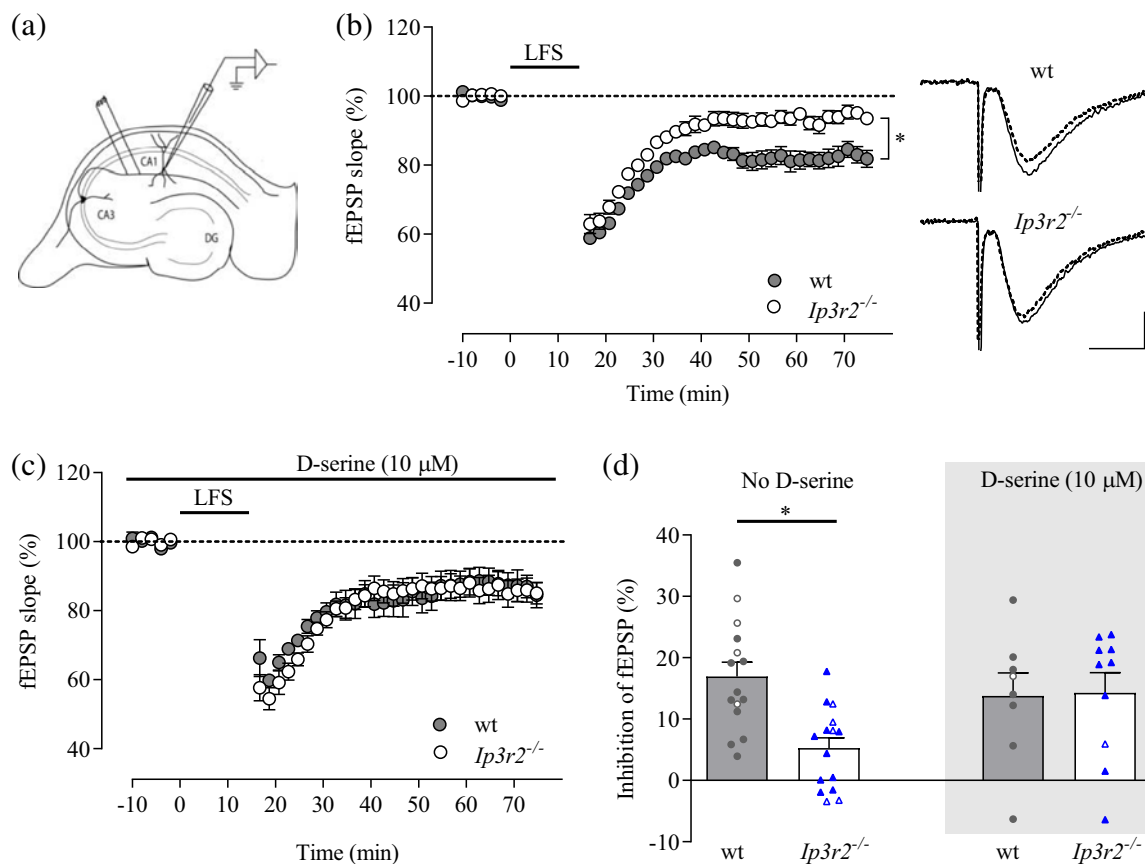


**FIGURE 5** Long-term depression was impaired in *Ip3r2*<sup>-/-</sup> animals. (a) Schematic representation of a transverse hippocampal slice showing the recording configuration used to obtain extracellular responses in the CA1 dendritic layer (*stratum radiatum*) evoked by stimulation of the Schaffer collateral fibers. (b) Experimental time course of the experiment, with each time point representing mean ± SEM. Insets on the right display fEPSPs taken from one wt and one *Ip3r2*<sup>-/-</sup> mice at baseline (solid line) and 1 h after LFS (dashed line). Traces are averages of eight consecutive individual responses. Scale bar: 0.25 mV, 10 ms. (c) Similar to (b), but in the presence of D-serine (10 μM) in the bathing solution. (d) Bar graph showing LTD experiments carried out in the absence and in the presence of D-serine (10 μM). Note that, on average, LTD was significantly less stable in *Ip3r2*<sup>-/-</sup> compared to wt mice (\**p* < .05), but when the experiments were carried out in the presence of D-serine (10 μM), this difference was not observed. Data represent mean ± SEM. Individual experiments are superimposed on bar graphs with open and closed symbols (circles, wt; triangles, *Ip3r2*<sup>-/-</sup> mice) representing females and males, respectively. fEPSP, field excitatory postsynaptic potentials; LTD, long-term synaptic depression; LFS, low-frequency stimulation [Color figure can be viewed at [wileyonlinelibrary.com](http://wileyonlinelibrary.com)]

$\pm 2\%$ ,  $n = 12\text{--}13$  mice,  $p < .05$ ). To rule out possible abnormalities in basal synaptic transmission in  $Ip3r2^{-/-}$  animals, we constructed input–output curves of fEPSPs obtained at increasing intensities (10–100  $\mu\text{A}$ ). We observed that fEPSP slopes scaled up with the number of fibers recruited (as indicated by the presynaptic fiber volley amplitude) in a similar manner in both genotypes (Figure S1a,b), confirming the absence of major perturbations in synaptic transmission reported in previous studies (Agulhon et al., 2010; Petravicz et al., 2008). We further observed that the presence of D-serine (10  $\mu\text{M}$ ) did not significantly affect the input–output relationship in any of the two genotypes (Figure S1 a,b). Next, we confirmed that the rescuing effect of D-serine on  $Ip3r2^{-/-}$  LTD was NMDAR-dependent: as expected, even if D-serine (10  $\mu\text{M}$ ) was present in the bathing solution, LFS failed to cause a significant long-term modification of synaptic strength when the NMDAR antagonist, D-AP5 (10  $\mu\text{M}$ ), was coapplied (Figure 6).

Next, we tested if the facilitation of LTD by exogenous D-serine application was sensitive to DAAO (0.1 U/mL), an enzyme that oxidizes D-amino acids, including D-serine, thus preventing its critical role on NMDAR activation. Unexpectedly, the superfusion of DAAO

(0.1 U/mL) triggered a quick and robust depression of synaptic transmission in all slices tested (Figure S2a), contrasting with the previously reported lack of effect (Mothet et al., 2006). DAAO-induced depression ( $32.4 \pm 10\%$ ,  $n = 3$ ; Figure S2a) was reversible, with the fEPSPs slopes returning to near baseline values following its washout from the bathing solution (Figure S2a). Although it was outside of the scope of the present work to further characterize this unexpected depressant action of DAAO, it is important to point out that it occurred through a mechanism unrelated to NMDAR activity, since DAAO (0.1 U/mL) still inhibited fEPSPs when we included the NMDAR agonist, D-AP5 (25  $\mu\text{M}$ ), in the bathing solution ( $n = 3$ ; Figure S2a). Consistently, in the group of experiments aiming to test if the facilitation of LTD by exogenous D-serine application was sensitive to DAAO, the co-superfusion of DAAO (0.1 U/mL) and D-serine (10  $\mu\text{M}$ ) was also responsible for a depression of synaptic transmission ( $40.0 \pm 3\%$ ,  $n = 5$ ; Figure S2b), prompting us to collect a new baseline before applying LFS. In these conditions, as Figure 6 shows, the magnitude of LFS-induced LTD in  $IP_3R2$  KO mice was still enhanced ( $26.4 \pm 2\%$ ,  $n = 5$ ) compared to that obtained in the absence of D-serine ( $p < .05$ ). In a separate group of experiments, we preincubated hippocampal slices with DAAO (0.1 U/mL) for at least 1 h before moving them to the recording chamber, where DAAO (0.1 U/mL) was also present. As Figure 6 shows, preincubation with DAAO (0.1 U/mL) per se significantly disrupted LTD in hippocampal slices prepared from wild-type mice ( $3.37 \pm 3\%$  change over baseline,  $n = 6$ ,  $p < .05$ ), confirming the critical role played by endogenous D-serine in this form of synaptic plasticity (Zhang et al., 2008). Noteworthy, the washout of DAAO (0.1 U/mL) from the bathing solution in these slices resulted in a robust facilitation of synaptic transmission ( $69.8 \pm 14\%$ ,  $n = 3$ ; Figure S2c), which is consistent with the inhibitory effect of this enzyme on fEPSPs described above. In the case of  $IP_3R2$  KO mice, when slices were preincubated with DAAO, D-serine (10  $\mu\text{M}$ ) did not significantly enhance LTD (Figures 6,  $10.7 \pm 4\%$  depression,  $n = 17$ ). Importantly, post hoc analysis showed significant differences ( $p < .05$ ) between female ( $2.7 \pm 6\%$ ,  $n = 8$ ) and male mice ( $17.8 \pm 3\%$ ,  $n = 9$ ) under these conditions (see section 4).

In a final group of experiments, we sought to investigate if the new role of  $IP_3R2$ -mediated signaling herein described would extend to synaptic depotentiation. Our rationale was that given the constant adjustments in synaptic strength that occur *in situ*, it would be of interest to understand if synapses that had been previously potentiated could also see their depotentiation affected by the lack of  $IP_3R2$ -mediated signaling. To that extent, we started by applying high-frequency stimulation at 100 Hz to the Schaffer collateral fibers (see section 2), in a way that reliably induced LTP. We observed that, as previously shown (Agulhon et al., 2010; Shigetomi et al., 2013), on average, the lack of  $IP_3R2$  did not significantly affect CA1 hippocampal LTP (Figure 7a). One hour after triggering LTP, we ran an LFS protocol (1 Hz, similar to that used in LTD experiments), to test synaptic depotentiation (Figure 7a). In line with our hypothesis, depotentiation was slightly, but significantly ( $n = 8\text{--}10$ ,  $p < .05$ ), facilitated when  $IP_3R2$ -mediated signaling was intact (Figure 7b), further supporting the contribution of this predominantly nonneuronal mechanism to the neural correlates of long-term memory.

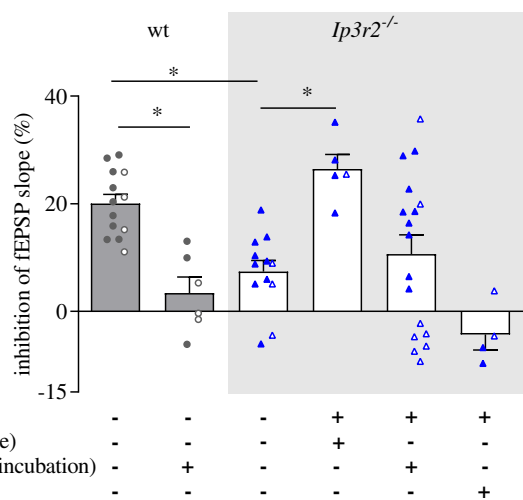


**FIGURE 6** D-serine was critical for LTD maintenance, rescuing  $Ip3r2^{-/-}$ -induced impairment in an NMDAR-dependent manner. Bar graph showing LTD experiments carried out in the absence or in the presence of D-serine (10  $\mu\text{M}$ ) alone or in combination with DAAO (0.1 U/mL, applied acutely or preincubated for >1 h) or with the NMDAR antagonist, D-AP5. “+” sign represents presence, and “-” represents the absence of the drug indicated on the lower left, below the bar graph. Note that, on average, LTD was virtually blocked ( $*p < .05$ ) in the wild type after preincubation with DAAO (0.1 U/mL). When applied acutely, DAAO did not prevent the significant ( $*p < .05$ ) enhancement of LTD in  $IP_3R2$ -deficient mice by exogenous D-serine. Conversely, D-serine did not significantly enhance LTD in  $IP_3R2$ -deficient mice when hippocampal slices were preincubated with DAAO, an effect that post hoc analysis revealed to be mostly driven by female mice. Note that the presence of D-AP5 blocked LTD. Data represent mean  $\pm$  SEM. Individual experiments are superimposed on bar graphs with open and closed symbols (circles, wt; triangles,  $Ip3r2^{-/-}$  mice) representing females and males, respectively. DAAO, D-amino acid oxidase; LTD, long-term synaptic depression [Color figure can be viewed at [wileyonlinelibrary.com](http://wileyonlinelibrary.com)]

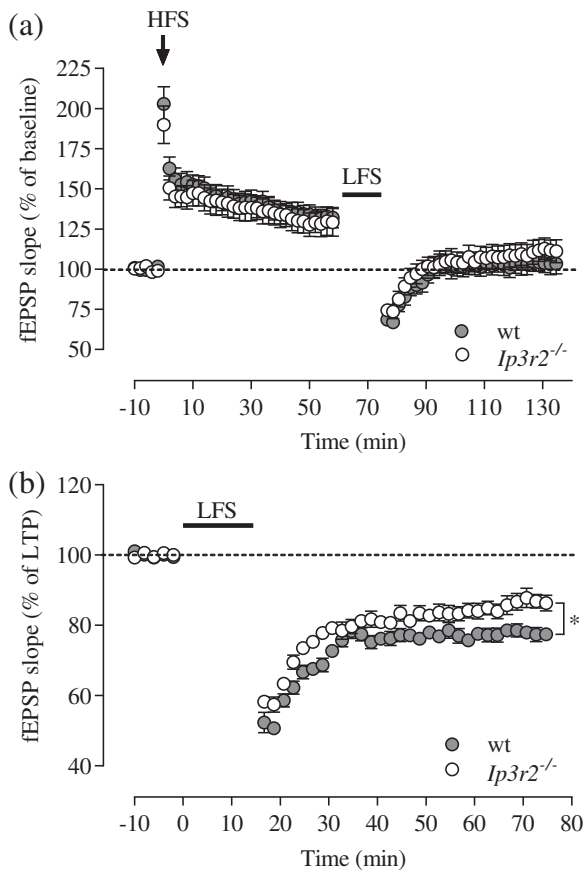


**FIGURE 7** Synaptic depotentiation was impaired in *Ip3r2*<sup>-/-</sup> animals. (a) Experimental time course of LTP / depotentiation experiments. (b) The experimental block pertaining to LFP-induced synaptic depotentiation was renormalized using the last 10 min of LTP as baseline. Note that, on average, LTP was not significantly different between *Ip3r2*<sup>-/-</sup> and wt mice (a), but *Ip3r2*<sup>-/-</sup> animals displayed significantly ( $p < .05$ ) impaired depotentiation (b). Data represent mean  $\pm$  SEM. LFS, low-frequency stimulation; LTD, long-term synaptic depression; HFS, high-frequency tetanic stimulation

## 4 | DISCUSSION

In this study, we showed that *Ip3r2*<sup>-/-</sup> mice exhibited significant impairments in long-term memory. Those deficits were exclusive of remote, and not recent, memory. Further, they were not restricted to recognition memory, as in the case of the GFAP–TeNT mouse (Lee et al., 2014), but instead had a more generalized impact upon remote memory function. It is likely that such broader consequences result from IP<sub>3</sub>R2-mediated signaling being upstream of TeNT-sensitive vesicle release. Specifically, when compared to wt littermates, IP<sub>3</sub>R2-deficient mice presented an impoverished performance in remote NOR and remote fear memory. *Ip3r2*<sup>-/-</sup> animals also made significantly more errors in the retention task of the Barnes maze, a result that supports a deficit in remote spatial memory. Contrasting with the IP<sub>3</sub>R2 KO, the performance of wild-type controls in the Barnes maze after a 2–4 weeks delay was, in fact, better than on the last day of training, suggesting that IP<sub>3</sub>R2-mediated Ca<sup>2+</sup> signaling played an important role in memory consolidation with the

passage of time (Vertes, 2004). It is noteworthy that littermates of both sexes were used in our experiments, and while alterations in remote memory related to the lack of IP<sub>3</sub>R2 could be found in female and male mice, those differences were reflected in different ways across behavioral tests. Future studies will be necessary to explore further potential sex differences associated with IP<sub>3</sub>R2-mediated signaling and memory.

It is thought that memory consolidation processes are optimally engaged when the molecular signals that mediate LTP-related synaptic remodeling are suppressed and LTD-related signaling is enhanced (Vyazovskiy et al., 2008). Consistently, we found that the absence of IP<sub>3</sub>R2-mediated signaling significantly disrupted hippocampal NMDA-receptor dependent LTD, compared with wt littermate controls. The LTD impairment observed in IP<sub>3</sub>R2-deficient mice might thus perturb memory consolidation, as proposed in the synaptic scaling hypothesis (Tononi & Cirelli, 2003), causing, at least in part, the cognitive deficiencies observed. In light of such a hypothesis, IP<sub>3</sub>R2-mediated signaling could play an important role in the homeostatic mechanisms that participate in the downscaling of synaptic strength and consequently lead to the amplification of the signal-to-noise ratio of potentiated synapses. Because our experiments further showed that IP<sub>3</sub>R2-mediated signaling facilitated synaptic depotentiation, one can postulate that astrocytes might help fine-tune information for long-term storage by dynamically readjusting synaptic strengths.

Memory consolidation is thought to also involve the generation of hippocampal high-frequency (150–250 Hz) transient oscillations (~100 ms), termed sharp-wave ripples (SWRs), during slow-wave sleep (SWS), and in the awake state during consummation and immobility (Buzsáki, 2015). SWRs coincide with the reactivation of the hippocampus as a result of recent behavioral experiences and are thought to facilitate the hippocampal–neocortical interactions necessary for transferring and integrating newly encoded memories into pre-existing knowledge cortical networks (Buzsáki, 1998; Diekelmann & Born, 2010; Lee & Wilson, 2002). Recent results by Tang et al. (2017) strengthened the hypothesis that SWRs occurring during SWS are particularly suited to support memory consolidation. Interestingly, while SWRs were shown to occur at longer intervals in IP<sub>3</sub>R2 KO compared to wild-type mice in urethane-anesthetized mice (Tanaka et al., 2017), the attenuation of IP<sub>3</sub>/Ca<sup>2+</sup> signaling in astrocytes did not cause significant alterations in SWS in nonanesthetized mice (Foley et al., 2017). In light of those results, further investigations will be necessary to determine the physiological relevance of IP<sub>3</sub>R2-dependent modulation of SWRs under anesthesia.

Our experiments further showed that IP<sub>3</sub>R2-mediated Ca<sup>2+</sup> impairment of LTD could be rescued upon application of exogenous D-serine. It is not the first time that the lack of IP<sub>3</sub>R2 is linked to an attenuation of D-serine levels: Takata et al. (2011) showed that D-serine release upon stimulation of a main cholinergic projection to the hippocampus was significantly reduced in IP<sub>3</sub>R2 KOs compared to wild-type mice. Noteworthy, we did not observe LTD impairments in a previous study using a transgene mouse in which the inducible expression of tetanus toxin disrupted vesicle release exclusively in astrocytes. It is thus possible that the attenuation of D-serine levels in

the IP<sub>3</sub>R2 KO stems, at least in part, from impairments in mechanisms other than vesicular release. Although it was outside of the scope of our present study to identify those, one interesting possibility is that the lack of IP<sub>3</sub>R2-mediated signaling affects the synthesis of L-serine in astrocytes and/or its shuttle from astrocytes into neurons, where it is converted to D-serine.

Astrocytes' contribution to information processing through homosynaptic depression is consistent with previous evidence that either their chemical inactivation with sodium fluoroacetate or the degradation of endogenous D-serine by DAAO impaired NMDAR-dependent LTD (Zhang et al., 2008). In our experiments, DAAO also occluded NMDAR-dependent LTD in wild-type mice. Further, preincubation with this enzyme prevented the rescuing effect of D-serine on IP<sub>3</sub>R2 KO LTD. Importantly, post hoc analysis suggested that such an effect was mostly driven by female mice. While future studies will be necessary to better understand why that might be the case, our observations add additional evidence to the growing body of literature showing a strong sex-dependence of DAAO actions in the rodent brain (Labrie et al., 2009; Pritchett et al., 2015), as well as sex-related differences in its expression levels in humans (Jagannath et al., 2017). Moreover, our results indicating that female mice are more sensitive than males to the disruption of D-serine actions in the brain, are well aligned with previous reports showing the inability of DAAO to prevent the facilitatory actions of exogenously applied D-serine on LTD (Zhang et al., 2008) or LTP (Yang et al., 2003) in male rodents.

It is noteworthy that the lack of IP<sub>3</sub>R2 did not produce obvious alterations in the health of our mice, including in coat condition, in apparent contrast with a previous study (Cao et al., 2013). However, important differences between the two studies might account for such a discrepancy. While we looked for possible differences in fur color, wounds or patchy fur as part of a routine health check before starting the behavioral screening, it was not our goal to quantify the ability of individual mice to groom different body regions across several days or weeks, as performed by Cao et al. (2013). Further investigations might be useful to gain a better understanding of these and other differences, and also to identify eventual additional phenotypes. For example, it seems relevant to investigate whether impairments in other synaptic mechanisms, such as in heterosynaptic cholinergic-mediated LTP in the hippocampus (Navarrete et al., 2012) and in cortex (Takata et al., 2011), which were demonstrated to occur in the IP<sub>3</sub>R2 KO, might be responsible for specific behavioral alterations. It also seems important to determine why mice expressing an IP<sub>3</sub> absorbent "IP<sub>3</sub> sponge" showed impairments in recent spatial memory in connection with glutamate spillover and the retraction of astrocytic processes (Tanaka et al., 2013), but similar morphological alterations (Perez-Alvarez et al., 2014) and behavioral deficits (our study) were not observed in IP<sub>3</sub>R2 KO mice. In fact, in the IP<sub>3</sub>R2 KO, ambient glutamate concentration and tonic NMDAR activation were shown to be largely preserved (Petraevicz et al., 2008).

In conclusion, our results showing that IP<sub>3</sub>R2-mediated signaling has a facilitatory effect on long-term memory in vivo provide an important new insight into the key roles of astrocytic Ca<sup>2+</sup> signals on neural circuits function and cognitive behavior. Despite the specific

differences between the "IP<sub>3</sub> sponge" model (Tanaka et al., 2013) and the IP<sub>3</sub>R2 KO that was used here and by others (Navarrete et al., 2012; Takata et al., 2011), converging evidence indicates that IP<sub>3</sub>R2 activation leads to a downstream modulation of synaptic transmission and plasticity that favors normal cognitive behaviors. It is likely that all of the effects resulting from IP<sub>3</sub>R2-mediated signaling act together to increase the flexibility and information storage capacity of the brain (Dayan & Willshaw, 1991), making it challenging to assess the relative contribution of each of those modifications individually. With that in mind, we propose that IP<sub>3</sub>R2-dependent astrocytic Ca<sup>2+</sup> signaling can help modulate synaptic strength bidirectionally (positively or negatively), as necessary to optimize information transmission and its long-term storage in neuronal networks.

## ACKNOWLEDGMENTS

We warmly thank Dr. Catarina C. Fernandes for her outstanding scientific input, Dr. Ju Chen and Dr. Axel Nimmerjahn for making available the mice used in this study and Mr. Joseph Chambers for his invaluable technical assistance. We further thank Dr. T. K. Booker Porter for helpful advice, Dr. Sora Shin for constructive comments on a previous version of this manuscript, Dr. Margarita M. Behrens for encouragement and Mr. Jorge Aldana for exceptional IT support. This work and A.P.-D. received support from the Kavli Institute for Brain and Mind (KIBM Innovative Research Grant #2015-047) and the Calouste Gulbenkian Foundation. K.O. is supported by the Shenzhen Basic Research Foundation (KCYJ20160428154108239, KQJSCX20170330155020267). T.J.S. was supported by the Howard Hughes Medical Institute.

## CONFLICT OF INTEREST

The authors have no conflict of interest in relation to the work herein described.

## ORCID

António Pinto-Duarte  <https://orcid.org/0000-0002-2215-7653>

Amanda J. Roberts  <https://orcid.org/0000-0002-4044-8884>

Kunfu Ouyang  <https://orcid.org/0000-0003-0292-375X>

Terrence J. Sejnowski  <https://orcid.org/0000-0002-0622-7391>

## REFERENCES

- Agulhon, C., Fiocco, T. A., & McCarthy, K. D. (2010). Hippocampal short- and long-term plasticity are not modulated by astrocyte Ca<sup>2+</sup> signaling. *Science*, 327, 1250–1254.
- Anderson, W. W., & Collingridge, G. L. (2007). Capabilities of the WinLTP data acquisition program extending beyond basic LTP experimental functions. *Journal of Neuroscience Methods*, 162, 346–356.
- Bear, M. F., & Abraham, W. C. (1996). Long-term depression in hippocampus. *Annual Review of Neuroscience*, 19, 437–462.
- Berridge, M. J. (1993). Inositol trisphosphate and calcium signalling. *Nature*, 361, 315–325.



- Bezzi, P., Gundersen, V., Galbete, J. L., Seifert, G., Steinhauser, C., Pilati, E., & Volterra, A. (2004). Astrocytes contain a vesicular compartment that is competent for regulated exocytosis of glutamate. *Nature Neuroscience*, *7*, 613–620.
- Broadbent, N. J., Gaskin, S., Squire, L. R., & Clark, R. E. (2010). Object recognition memory and the rodent hippocampus. *Learning & Memory*, *17*, 5–11.
- Buzsáki, G. (1998). Memory consolidation during sleep: A neurophysiological perspective. *Journal of Sleep Research*, *7*(Suppl 1), 17–23.
- Buzsáki, G. (2015). Hippocampal sharp wave-ripple: A cognitive biomarker for episodic memory and planning. *Hippocampus*, *25*, 1073–1188.
- Cao, X., Li, L.-P., Wang, Q., Wu, Q., Hu, H.-H., Zhang, M., ... Gao, T.-M. (2013). Astrocyte-derived ATP modulates depressive-like behaviors. *Nature Medicine* [Internet], *19*, 773–777.
- Di Castro, M. A., Chuquet, J., Liaudet, N., Bhaukaurally, K., Santello, M., Bouvier, D., ... Volterra, A. (2011). Local  $Ca^{2+}$  detection and modulation of synaptic release by astrocytes. *Nature Neuroscience*, *14*, 1276–1284.
- Dayan, P., & Willshaw, D. J. (1991). Optimising synaptic learning rules in linear associative memories. *Biological Cybernetics*, *65*, 253–265.
- Diekelmann, S., & Born, J. (2010). The memory function of sleep. *Nature Reviews. Neuroscience*, *11*, 114–126.
- Dong, Z., Gong, B., Li, H., Bai, Y., Wu, X., Huang, Y., ... Wang, Y. T. (2012). Mechanisms of hippocampal long-term depression are required for memory enhancement by novelty exploration. *The Journal of Neuroscience*, *32*, 11980–11990.
- Fellin, T., Halassa, M. M., Terunuma, M., Succol, F., Takano, H., Frank, M., ... Haydon, P. G. (2009). Endogenous nonneuronal modulators of synaptic transmission control cortical slow oscillations in vivo. *Proceedings of the National Academy of Sciences of the United States of America*, *106*, 15037–15042.
- Fiacco, T. A., & McCarthy, K. D. (2004). Intracellular astrocyte calcium waves in situ increase the frequency of spontaneous AMPA receptor currents in CA1 pyramidal neurons. *The Journal of Neuroscience*, *24*, 722–732.
- Foley, J., Blutstein, T., Lee, S., Erneux, C., Halassa, M. M., & Haydon, P. (2017). Astrocytic IP<sub>3</sub>/Ca<sup>2+</sup> signaling modulates theta rhythm and REM sleep. *Frontiers in Neural Circuits*, *11*(3).
- Foskett, J. K., White, C., Cheung, K.-H., & D-OD, M. (2007). Inositol trisphosphate receptor  $Ca^{2+}$  release channels. *Physiological Reviews*, *87*, 593–658.
- Ge, Y., Dong, Z., Bagot, R. C., Howland, J. G., Phillips, A. G., Wong, T. P., & Wang, Y. T. (2010). Hippocampal long-term depression is required for the consolidation of spatial memory. *Proceedings of the National Academy of Sciences of the United States of America*, *107*, 16697–16702.
- Gimenez, E., & Montoliu, L. (2001). A simple polymerase chain reaction assay for genotyping the retinal degeneration mutation (Pdeb(rd1)) in FVB/N-derived transgenic mice. *Laboratory Animals*, *35*, 153–156.
- Holtzclaw, L. A., Pandhit, S., Bare, D. J., Mignery, G. A., & Russell, J. T. (2002). Astrocytes in adult rat brain express type 2 inositol 1,4,5-trisphosphate receptors. *Glia*, *39*, 69–84.
- Jagannath, V., Marinova, Z., Monoranu, C.-M., Walitza, S., & Grünblatt, E. (2017). Expression of D-amino acid oxidase (DAO/DAAO) and D-amino acid oxidase activator (DAOA/G72) during development and aging in the human post-mortem brain. *Frontiers in Neuroanatomy*, *11*, 31.
- Jourdain, P., Bergersen, L. H., Bhaukaurally, K., Bezzi, P., Santello, M., Domercq, M., ... Volterra, A. (2007). Glutamate exocytosis from astrocytes controls synaptic strength. *Nature Neuroscience*, *10*, 331–339.
- Kol, A., Adamsky, A., Groysman, M., Kreisel, T., London, M., ... Goshen, I. (2019). Astrocytes Contribute to Remote Memory Formation by Modulating Hippocampal-Cortical Communication During Learning. *bioRxiv* [Internet]: 682344. Available from: <http://biorxiv.org/content/early/2019/06/26/682344.abstract>
- Labrie, V., Clapcote, S. J., & Roder, J. C. (2009). Mutant mice with reduced NMDA-NR1 glycine affinity or lack of d-amino acid oxidase function exhibit altered anxiety-like behaviors. *Pharmacology, Biochemistry, and Behavior*, *91*, 610–620.
- Lee, A. K., & Wilson, M. A. (2002). Memory of sequential experience in the hippocampus during slow wave sleep. *Neuron*, *36*, 1183–1194.
- Lee, H. S., Ghetti, A., Pinto-Duarte, A., Wang, X., Dziejczapolski, G., Galimi, F., ... Heinemann, S. F. (2014). Astrocytes contribute to gamma oscillations and recognition memory. *Proceedings of the National Academy of Sciences*, *111*, E3343–E3352.
- Li, H., Xie, Y., Zhang, N., Yu, Y., Zhang, Q., & Ding, S. (2015). Disruption of IP<sub>3</sub>R2-mediated  $Ca^{2+}$  signaling pathway in astrocytes ameliorates neuronal death and brain damage while reducing behavioral deficits after focal ischemic stroke. *Cell Calcium*, *58*, 565–576.
- Li, X., Zima, A. V., Sheikh, F., Blatter, L. A., & Chen, J. (2005). Endothelin-1-induced arrhythmic  $Ca^{2+}$  signaling is abolished in atrial myocytes of inositol-1,4,5-trisphosphate(IP<sub>3</sub>)-receptor type 2-deficient mice. *Circulation Research*, *96*, 1274–1281.
- Marshall, L., Born, J. (2007). The contribution of sleep to hippocampus-dependent memory consolidation. *Trends Cogn Sci*, *11*, 442–450.
- Mikoshiba, K. (2007). IP<sub>3</sub> receptor/ $Ca^{2+}$  channel: From discovery to new signaling concepts. *Journal of Neurochemistry*, *102*, 1426–1446.
- Mothet, J. P., Rouaud, E., Sinet, P.-M., Potier, B., Jouvenceau, A., Dutar, P., ... Billard, J.-M. (2006). A critical role for the glial-derived neuro-modulator d-serine in the age-related deficits of cellular mechanisms of learning and memory. *Aging Cell*, *5*, 267–274.
- Navarrete, M., Perea, G., Maglio, L., Pastor, J., García De Sola, R., & Araque, A. (2013). Astrocyte calcium signal and gliotransmission in human brain tissue. *Cerebral Cortex*, *23*, 1240–1246.
- Navarrete, M., Perea, G., de Sevilla, D. F., Gómez-Gonzalo, M., Núñez, A., Martín, E. D., & Araque, A. (2012). Astrocytes mediate in vivo cholinergic-induced synaptic plasticity. *PLoS Biology*, *10*(2), e1001259.
- Okubo, Y., Kanemaru, K., Suzuki, J., Kobayashi, K., Hirose, K., & Iino, M. (2019). Inositol 1,4,5-trisphosphate receptor type 2-independent  $Ca^{2+}$  release from the endoplasmic reticulum in astrocytes. *Glia*, *67*, 113–124.
- Panatier, A., Vallée, J., Haber, M., Murai, K. K., Lacaille, J. C., & Robitaille, R. (2011). Astrocytes are endogenous regulators of basal transmission at central synapses. *Cell*, *146*, 785–798.
- Perez-Alvarez, A., Navarrete, M., Covelo, A., Martín, E. D., & Araque, A. (2014). Structural and functional plasticity of astrocyte processes and dendritic spine interactions. *The Journal of Neuroscience*, *34*, 12738–12744.
- Petravicz, J., Boyt, K. M., & McCarthy, K. D. (2014). Astrocyte IP<sub>3</sub>R2-dependent  $Ca^{2+}$  signaling is not a major modulator of neuronal pathways governing behavior. *Frontiers in Behavioral Neuroscience*.
- Petravicz, J., Fiacco, T. A., McCarthy, K. D., Navarrete, M., Perea, G., de Sevilla, D. F., ... McCarthy, K. D. (2008). Loss of IP<sub>3</sub> receptor-dependent  $Ca^{2+}$  increases in hippocampal astrocytes does not affect baseline CA1 pyramidal neuron synaptic activity. *The Journal of Neuroscience*, *28*, 4967–4973.
- Pritchett, D., Hasan, S., Tam, S. K. E., Engle, S. J., Brandon, N. J., Sharp, T., ... Peirson, S. N. (2015). D-amino acid oxidase knockout (*Dao*<sup>-/-</sup>) mice show enhanced short-term memory performance and heightened anxiety, but no sleep or circadian rhythm disruption. *The European Journal of Neuroscience*, *41*, 1167–1179.
- Sharp, A. H., Nucifora, F. C., Jr., Blondel, O., Sheppard, C. A., Zhang, C., Snyder, S. H., ... Ross, C. A. (1999). Differential cellular expression of isoforms of inositol 1,4,5-trisphosphate receptors in neurons and glia in brain. *The Journal of Comparative Neurology*, *406*, 207–220.
- Sherwood, M. W., Arizono, M., Hisatsune, C., Bannai, H., Ebisui, E., Sherwood, J. L., ... Mikoshiba, K. (2017). Astrocytic IP<sub>3</sub>Rs: Contribution to  $Ca^{2+}$  signalling and hippocampal LTP. *Glia*, *65*, 502–513.
- Shigetomi, E., Jackson-Weaver, O., Huckstepp, R. T., O'Dell, T. J., & Khakh, B. S. (2013). TRPA1 channels are regulators of astrocyte basal

- calcium levels and long-term potentiation via constitutive D-serine release. *The Journal of Neuroscience*, 33, 10143–10153.
- Takata, N., Mishima, T., Hisatsune, C., Nagai, T., Ebisui, E., Mikoshiba, K., & Hirase, H. (2011). Astrocyte calcium signaling transforms cholinergic modulation to cortical plasticity in vivo. *The Journal of Neuroscience*, 31, 18155–18165.
- Tanaka, M., Shih, P.-Y., Gomi, H., Yoshida, T., Nakai, J., Ando, R., ... Itohara, S. (2013). Astrocytic  $Ca^{2+}$  signals are required for the functional integrity of tripartite synapses. *Molecular Brain*, 595, 6557–6568.
- Tanaka, M., Wang, X., Mikoshiba, K., Hirase, H., & Shinohara, Y. (2017). Rearing-environment-dependent hippocampal local field potential differences in wild-type and inositol trisphosphate receptor type 2 knock-out mice. *The Journal of Physiology*, 595, 6557–6568.
- Tang, W., Shin, J. D., Frank, L. M., & Jadhav, S. P. (2017). Hippocampal-prefrontal reactivation during learning is stronger in awake compared with sleep states. *The Journal of Neuroscience*, 37, 11789–11805.
- Taylor, C. W., & Tovey, S. C. (2010). IP<sub>3</sub> receptors: Toward understanding their activation. *Cold Spring Harbor Perspectives in Biology*, 2, a004010.
- Tononi, G., & Cirelli, C. (2003). Sleep and synaptic homeostasis: A hypothesis. *Brain Research Bulletin*, 62, 143–150.
- Tononi, G., & Cirelli, C. (2006). Sleep function and synaptic homeostasis. *Sleep Medicine Reviews*, 10, 49–62.
- Vertes, R. P. (2004). Memory consolidation in sleep. *Neuron*, 44, 135–148.
- Vyazovskiy, V. V., Cirelli, C., Pfister-Genskow, M., Faraguna, U., & Tononi, G. (2008). Molecular and electrophysiological evidence for net synaptic potentiation in wake and depression in sleep. *Nature Neuroscience*, 11, 200–208.
- Yang, Y., Ge, W., Chen, Y., Zhang, Z., Shen, W., Wu, C., ... Duan, S. (2003). Contribution of astrocytes to hippocampal long-term potentiation through release of D-serine. *Proceedings of the National Academy of Sciences of the United States of America*, 100, 15194–15199.
- Zhang, Z., Gong, N., Wang, W., Xu, L., & Xu, T. (2008). Bell-shaped d-serine actions on hippocampal long-term depression and spatial memory retrieval. *Cerebral Cortex*, 18, 2391–2401.
- Zorec, R., Verkhratsky, A., Rodríguez, J. J., & Parpura, V. (2016). Astrocytic vesicles and gliotransmitters: Slowness of vesicular release and synaptobrevin2-laden vesicle nanoarchitecture. *Neuroscience*, 323, 67–75.

## SUPPORTING INFORMATION

Additional supporting information may be found online in the Supporting Information section at the end of this article.

**How to cite this article:** Pinto-Duarte A, Roberts AJ, Ouyang K, Sejnowski TJ. Impairments in remote memory caused by the lack of Type 2 IP<sub>3</sub> receptors. *Glia*. 2019;67: 1976–1989. <https://doi.org/10.1002/glia.23679>